Received: 13 September 2019 | Revised: 26 November 2019 | Accepted: 5 December 2019

DOI: 10.1096/fj.201902352R

RESEARCH ARTICLE

THE FASEB JOURNAL

Metabolic changes related to the IDH1 mutation in gliomas preserve TCA-cycle activity: An investigation at the protein level

Lennard J. M. Dekker[1] | Suying Wu[1] | Cherise Jurriëns[1] | Dana A. N. Mustafa[2] | Frederieke Grevers[2] | Peter C. Burgers[1] | Peter A. E. Sillevis Smitt[1] | Johan M. Kros[2] | Theo M. Luider[1]

[1]Department of Neurology, Erasmus University Medical Centre Rotterdam, Rotterdam, the Netherlands

[2]Department of Pathology, Erasmus University Medical Centre Rotterdam, Rotterdam, the Netherlands

Correspondence
Theo M. Luider, Laboratories of Neuro-Oncology/Clinical and Cancer Proteomics, Department of Neurology, Erasmus University Medical Centre Rotterdam, P.O. Box 2040, Rotterdam 3000 CA, the Netherlands.
Email: t.luider@erasmusmc.nl

Funding information
The mass spectrometry equipment used for this publication is (partly) financed by the Netherlands Organisation for Scientific Research (NWO) infrastructure grant number 1631. This work has received funding from the Eurostars-2 joint program with co-funding from the European Union Horizon 2020 research and innovation program (Eurostars project 10688 (GlioPhos)) and by the British Brain Tumour Charity (GN-000540)

Abstract

The discovery of the IDH1 R132H (IDH1 mut) mutation in low-grade glioma and the associated change in function of the IDH1 enzyme has increased the interest in glioma metabolism. In an earlier study, we found that changes in expression of genes involved in the aerobic glycolysis and the TCA cycle are associated with IDH1 mut. Here, we apply proteomics to FFPE samples of diffuse gliomas with or without IDH1 mutations, to map changes in protein levels associated with this mutation. We observed significant changes in the enzyme abundance associated with aerobic glycolysis, glutamate metabolism, and the TCA cycle in IDH1 mut gliomas. Specifically, the enzymes involved in the metabolism of glutamate, lactate, and enzymes involved in the conversion of α-ketoglutarate were increased in IDH1 mut gliomas. In addition, the bicarbonate transporter (SLC4A4) was increased in IDH1 mut gliomas, supporting the idea that a mechanism preventing intracellular acidification is active. We also found that enzymes that convert proline, valine, leucine, and isoleucine into glutamate were increased in IDH1 mut glioma. We conclude that in IDH1 mut glioma metabolism is rewired (increased input of lactate and glutamate) to preserve TCA-cycle activity in IDH1 mut gliomas.

KEYWORDS

glioma, glutaminolysis, IDH1 mutation, metabolism, proteomics, TCA cycle

1 | INTRODUCTION

Mutations in isocitrate dehydrogenase (IDH) 1 and 2 occur in the majority of diffuse infiltrating gliomas. The IDH1 R132H mutation (IDH1 mut) is present in approximately 80% of grade II-III gliomas and secondary glioblastoma that progressed from low-grade astrocytoma.[1] Mutations in IDH2 are much less common and are mutually exclusive with mutations in IDH1. IDH1 and IDH2 mutations are specific to codons that encode for arginine, an important amino acid in the catalytic domain of these enzymes. Most IDH1 mutations have been identified at the Arg132 codon (R132), and mutations in IDH2 have

Abbreviations: ACACA, acetyl-CoA carboxylase 1; DDA, data-dependent acquisition; DTT, dithiothreitol; ECHS1, enoyl-CoA hydratase; FASN, fatty acid synthase; FFPE, formalin fixed paraffin embedded; IAA, iodoacetamide; IDH ½, isocitrate dehydrogenase 1 and 2; MLYCD, malonyl-CoA decarboxylase; NCE, normalized collision energy; PDX, patient-derived xenograft; SDC, sodium deoxycholate; TCA, tricarboxylic acid.

This is an open access article under the terms of the Creative Commons Attribution-NonCommercial-NoDerivs License, which permits use and distribution in any medium, provided the original work is properly cited, the use is non-commercial and no modifications or adaptations are made.
© 2020 The Authors. *The FASEB Journal* published by Wiley Periodicals, Inc. on behalf of Federation of American Societies for Experimental Biology

been identified at the Arg140 codon (R140) and Arg172 codon (R172).[2] Glioma patients with IDH1/2 mutations have a significantly better prognosis compared with patients without these mutations.[2] IDH1 and IDH2 mutations occur early in gliomagenesis and change the metabolic function of these enzymes. IDH1 mut leads to the production of excessive amounts of the oncometabolite 2-hydroxyglutarate (2-HG) in glioma cells.[3] The identification of the mutations in IDH1 and IDH2 and their relative positive effects on the prognosis compared with IDH1 wild-type (IDH1 wt) glioma patients has increased interest in glioma metabolism in the brain.

Multiple preclinical models have provided possibilities to study the oncogenic properties of IDH1/2 mutations compared with IDH1 wt. In these models epigenetic regulation, cancer cell differentiation, and metabolism are shown to be altered.[3] The IDH1 mut induces changes in the concentration of tricarboxylic acid (TCA) cycle intermediates and lipid metabolites.[4,5] In vitro and in vivo studies demonstrated that the inhibition of IDH1/2-mutant enzymes decreases intracellular D-2-hydroxyglutarate (D-2HG) levels and reverses epigenetic dysregulation.[6,7] Gene expression profiles of large cohorts of glioma and acute myeloid leukemia have shown that IDH1/2 mutant tumors display a distinct gene expression profile enriched for genes expressed in progenitor cells.[8] Metabolic flux analyses have shown that IDH1 mut render tumor cells more dependent on citrate and fatty acids under hypoxia as compared with IDH1 wt cells and this metabolic reprogramming results in decreased cell growth of IDH1 mut cells upon hypoxia.[9]

By quantitative PCR the RNA expression of the enzymes part of the aerobic glycolysis and the TCA cycle were previously studied. The RNA expressional changes were found in the enzymes of the TCA cycle (increased) and aerobic glycolysis (LDHA decreased and LDHB increased).[10] More recently, a relationship between the IDH1 mut and lactate and glutamate dependency in glioma has been proposed.[11,12] Based on targeted RNA sequencing of a large series of metabolic enzymes, it was shown that enzymes transporting glutamate and lactate into the cell and enzymes converting lactate and glutamate into α-ketoglutarate are upregulated in IDH1 mut gliomas.[11] It was suggested that IDH1 mut gliomas depend on lactate and glutamate as metabolic substrates to alleviate metabolic stress as a result of defective isocitrate processing.[11]

In this study we validate previously obtained RNA expression data at the protein level and in addition studied the pentose phosphate pathway, TCA cycle, aerobic glycolysis, glutaminolysis, fatty acid metabolism, GABA shunt, and amino acid catabolism. To perform the proteomics mapping of the pathways, FFPE tissue samples of astrocytomas, oligodendrogliomas and GBMs were investigated. The samples were analyzed using both data-dependent analysis (DDA) and targeted mass spectrometry. First, data-dependent LC-MS analyses were performed to obtain a general overview of the abundance of proteins in the samples and to identify the most prominent differences in metabolic enzymes between IDH1 mut and wild-type tumors. Subsequently, the DDA data were used to develop a targeted semiquantitative multiplex method for 64 proteins related to the various metabolic pathways to obtain insight in the metabolic consequences of the IDH1 mutation. We observed that in IDH1 mut gliomas the enzymes of the aerobic glycolysis, glutaminolysis, and amino acid catabolism were most affected.

2 | MATERIALS AND METHODS

Unless otherwise noted, all chemicals were purchased from Sigma-Aldrich (Saint Louis, MO) and all solvents were purchased from Biosolve (Valkenswaard, The Netherlands).

2.1 | Samples

FFPE tissue samples of surgically resected gliomas from 48 patients were used. All these gliomas are classified based on the most recent guidelines provided by WHO.[13] The set included 18 astrocytomas (IDH1 R132H and TP53 mutated), 11 oligodendroglioma (IDH1 R132H and 1p/19q loss), and 19 GBM (IDH1 wt). Additional patient characteristics can be found in Table 1. The use of patient material was approved by the Institutional Review Board of the Erasmus MC, Rotterdam, the Netherlands (nr MEC 221.520/2002/262; date of approval 22 July 2003, and MEC-2005-057, date of approval 14 February 2005). Patients gave written informed consent to use their tissue for research purposes.

2.2 | Sample preparation

H&E stained sections of 4 μm were microscopically assessed for at least 70% tumor cells. For proteomic analyses adjacent

TABLE 1 Patient data

Groups	Grade	Average age (min-max)	IDH1 R132H	1p 19q co-deletion	TP53 mutation
Astrocytoma (n = 18)	II(12), III(6)	43.6 (27-68)	18	0	18
GBM primary (n = 19)	IV(19)	51.9 (29-69)	0	0	7
Oligodendroglioma (n = 11)	II(11)	49.3 (34-61)	11	11	1

8 μm sections were collected in LoBind Eppendorf tube. The tissue section was de-paraffinized by xylene (98%), hydrated with different concentrations of ethanol, sequentially 100%, 70%, 50%, and 0%, and all steps were followed by centrifugation with an Eppendorf centrifuge at maximum speed for 5 minutes. After each step the supernatant was discarded before proceeding to the next step. After the final step the samples were stored at −80°C until the time of digestion. To all samples 100 μL lysis buffer was added containing 1% SDC (sodium deoxycholate) in 0.3 M Tris (pH 8). The samples were disrupted by sonification for 2 min at 70% amplitude at a maximum temperature of 25°C (Branson, Ultrasonic, Danbury, CT). Subsequently, the samples were incubated for 90 minutes at 90°C. Five microliter of 0.1 M DTT (dithiothreitol) was added to the samples and incubated for 30 minutes at 60°C. Subsequently, 5 μL of 375 mM IAA (iodoacetamide) was added and incubated at room temperature for 30 minutes in a dark environment. Next, 300 ng of trypsin (Promega, Madison, WI) was added to each sample and after overnight incubation at 37°C, 2.5 μL 25% TFA was added to each sample and centrifuged at 20,000 *g* for 30 minutes. Supernatants of all samples were transferred to a 96 well plate and desalted. For the automated sample processing the Assay MAP Bravo platform (Agilent technologies, Santa Clara, CA) was used. C18 cartridges were primed with 100 μL 50% ACN/ 0.1% TFA and equilibrated with loading buffer (0.1% TFA/water). Hundred microliter of sample was loaded onto the C18 cartridge. After washing the cartridges with 100 μL loading buffer, the desalted peptides were eluted in 25 μL elution buffer: 70% ACN/0.1% TFA. Subsequently, the samples were dried using a vacuum centrifuge (Savant SC210A, Thermo Fisher Scientific). Samples were dissolved in 120 μL aqueous 0.1% TFA and the total volume of each sample was divided over five 96 well plates. Next, plates were sealed and stored at 4°C until the LC-MS measurements were performed.

2.3 | Nano-LC data-dependent mass spectrometry measurements

Samples were analyzed by nano-LC (Ultimate 3000RS, Thermo Fisher Scientific, Germering, Germany) coupled to a Q Exactive HF mass spectrometer (Thermo Fisher Scientific, Bremen, Germany). The samples were analyzed with the same method and settings as described previously.[14] The LC-MS/MS proteomics data was deposited to the ProteomeXchange Consortium via the PRIDE partner repository with the dataset identifier PXD016697.

2.4 | PRM measurements

PRM analyses were performed on the same nano-LC Orbitrap Q Exactive HF system as the DDA measurements. A shorter 30 minutes gradient is used on the nano-LC system under similar LC conditions as for the DDA measurements. A quadrupole isolation window of 0.6 m/z units, an AGC target of 1×10^6 ions, a maximum fill time of 120 ms, and an Orbitrap resolving power of 60,000 at 200 m/z were used. A normalized collision energy (NCE) of 27% was used for all peptides together with a retention time window of 4 minutes for each peptide. Eventually, the results for all proteins were evaluated and for each protein the two best performing peptides were selected. Targeted MS/MS methods could be successfully developed for 117 peptides belonging to 64 proteins (see Table S1). It was not possible to analyze all targets in a single method with the required sensitivity and retention time window. For this reason different methods were created, all containing a subset of the targeted peptides. The LC-MS/MS PRM proteomics data was deposited to the ProteomeXchange Consortium via the PRIDE partner repository with the dataset identifier PXD016698.

2.5 | Data processing and analysis DDA

MaxQuant 1.6.1.0 (http://www.coxdocs.org/doku.php?xml:id=maxquant:start) was used to analyze the DDA data; default settings were used unless indicated otherwise. All raw files were loaded and the human subset of the uniprot_sprot_2015-10 database was selected; Homo sapiens species restriction; 20,194 sequences, a maximum of two miss cleavages, oxidation as a variable modification of methionine, carbamidomethylation as a fixed modification of cysteine, and trypsin was set as enzyme. The label free quantitation option with matching between runs was used. The quantitative values for all identified protein groups were further analyzed in Perseus 1.6.1.2 (http://www.coxdocs.org/doku.php?xml:id=perseus:start). The data were annotated, log2 transformed, and imputation (replace value from normal distribution) was applied for missing values. Subsequently, hierarchical clustering and statistical analyses were performed to generate both heat maps and volcano plots.

2.6 | Data processing and analysis PRM data

The PRM data were analyzed using Skyline version 3.5.0.9320 MacCoss Lab Software, Seattle, WA (https://skyline.gs.washington.edu/labkey/project/home/software/Skyline/begin.view); fragment ions for each targeted mass were extracted and peak areas were integrated. Each fragment ion was visually inspected for interference and only fragment ions without interference in the integrated area were used and summed for further analyses. For all peptides, the areas were exported to Excel and correlation plots of peptides from the same protein were created. The values for all targeted proteins were imported in Perseus where the same analyses were performed as mentioned above for the DDA data.

3 | RESULTS

The LC-MS analyses of 18 astrocytomas (IDH1 R132H and TP53 mutated), 11 oligodendroglioma (IDH1 mut and 1p/19q loss), and 17 GBM (IDH1 wt) resulted in the identification of 1,509 protein groups. A hierarchical clustering of this dataset yielded two main clusters largely overlapping with the IDH1 status (Figure 1). The first cluster consisted of all but one GBM sample (all IDH1 wt), and two IDH1 mut samples (one oligodendroglioma and one astrocytoma). The other main cluster consisted of the rest of the samples with the IDH1 mut (gliomas graded 2 and 3), while one GBM IDH1 wt was present. The tumor samples harboring the co-deletion of 1p/19q (defining oligodendroglioma) were not discerned.

Twenty-eight proteins with functions in glycolysis, pentose phosphate pathway, TCA cycle, aerobic glycolysis, glutaminolysis, fatty acid metabolism, GABA shunt, and catabolism of amino acids appeared to be differentially expressed between the IDH1 mut and IDH1 wt group (Figure 2). To more precisely map qualitative and quantitative differences in abundance between the two groups, a targeted PRM mass spectrometry method was developed for 70 selected proteins related to these pathways. The relative quantity of 64 of these 70 proteins could be determined by PRM. For 53 proteins the relative quantity was based on two peptides; for the other 11 proteins quantitation was based on a single peptide. The normalization of the data was performed on UV intensity and could be validated based on actin abundance. The actin abundance between the IDH1 wt group and the IDH1 mut group was not statistically significant. In the IDH1 wt group two outliers with a significant lower abundance of actin (ACTC1) were observed and these samples were excluded from the analyses.

Of the 64 proteins analyzed by PRM, the abundance of 48 was significantly different between the IDH1 mut and IDH1 wt sample group when applying an FDR correction of 0.05 (Figure 3 and Table 2). The ratio of the quantified enzymes between IDH1 mut and IDH1 wt sample group is shown in a scheme of the glycolysis, pentose phosphate pathway, TCA cycle, and the glutaminolysis metabolic pathways (Figure 4). The largest shifts in the abundance of enzymes between tumors with and without IDH1 mutation are observed in the glutaminolysis and aerobic glycolysis (Figure 5). The ratios between LDHA and LDHB (enzymes that are involved in pyruvate conversion into lactate and lactate into pyruvate, respectively) and the transporters that import and export lactate (SLC16A3 and SLC16A7, respectively) are shown in Figure 5A. The ratios of these enzymes indicate that LDHB and SLC16A7 are higher in abundance in contrast to LDHA and SLC16A3 in the IDH1 mut group. This indicates that lactate import and its conversion in pyruvate is increased in IDH1 mut gliomas if one assumes that the abundance of these enzymes is associated with the concentration of their substrates and products. Figure 6 shows the abundances of enzymes relating to the GABA shunt, fatty acid metabolism, valine, leucine, and isoleucine degradation (ABAT (GABA shunt)); ECHS1 and MLYCD (fatty acid metabolism); and BCKHA, BCKHB, and HIBCH (valine, leucine, and isoleucine degradation). The levels of these enzymes, except MLYCD, were significantly elevated in IDH1 mut gliomas. For MLYCD, a regulator of fatty acid metabolism, no difference was observed between the two groups.

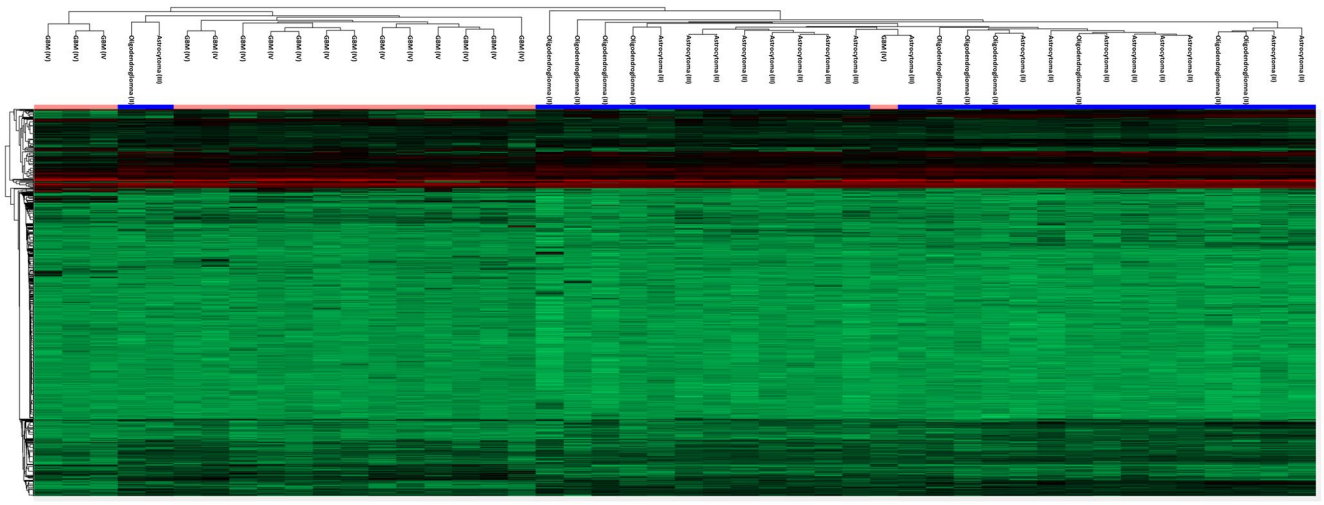

FIGURE 1 Heat map of DDA proteomics results of GBM, Astrocytoma, and Oligodendroglioma samples. Hierarchical clustering displayed as dendrograms. The protein abundances in each sample are represented as intensities log2 transformed and missing values were imputated by using background levels (a scale from red to green (high to low), pink = IDH1 wt, and blue = IDH1 mut)

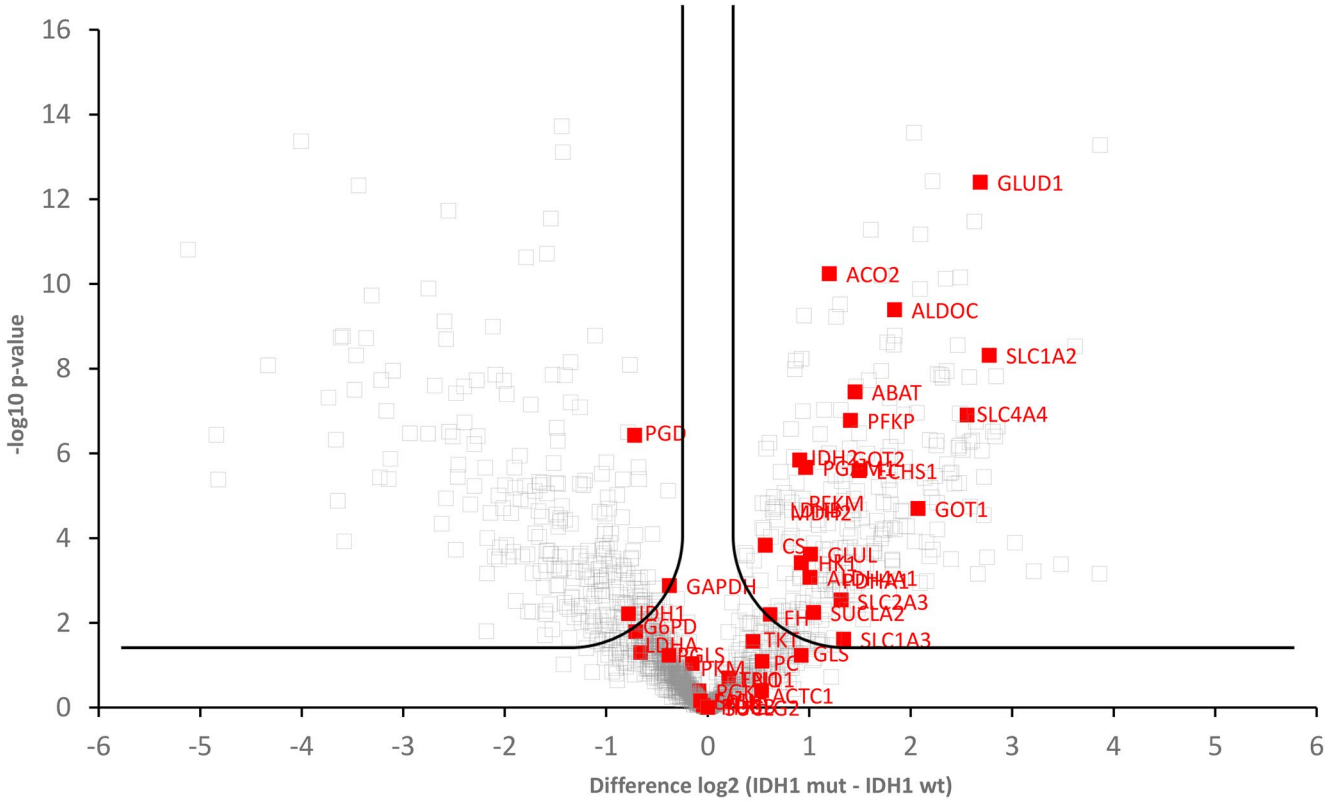

FIGURE 2 Volcano plot from DDA analyses. On the *x*-axis the difference in the log2 intensity values between IDH1 mut and IDH1 wt is indicated. The *y*-axis represents the −log10 of the *p*-value from the *t*-test. The cut-off is based on an FDR of 0.05 based on 250 randomizations of the dataset. The proteins related to the glycolysis, pentose phosphate pathway, TCA cycle, glutaminolysis, fatty acid metabolism, GABA shunt, and amino acid catabolism are labeled and marked in red

4 | DISCUSSION

Previously, we showed that RNA expression levels of aerobic glycolysis and the TCA-cycle enzymes change in IDH1 mut compared with IDH1 wt glioma.[10] In this study we confirmed these changes on the protein level. In addition, we included a number of connecting pathways to obtain a more complete view of the metabolic effects of these changes. To this end proteins of glycolysis, pentose phosphate pathway, aerobic glycolysis, fatty acid metabolism, GABA shunt, and catabolism of amino acids were included in our analyses. The most dominant changes between IDH1 mut and IDH1 wt gliomas were observed in enzymes and transporter proteins related to aerobic glycolysis and glutaminolyses. These observations confirm the previous findings at the RNA level[10-12] and strengthen the theory that both glutamate and lactate are imported and converted into α-ketoglutarate in IDH1 mut gliomas, to decrease metabolic stress caused by the mutation.[10-12] The increased import of lactate in IDH1 mut glioma cells results in a lower intracellular pH of tumor cells. Intracellular pH is tightly regulated in the cytoplasm within a narrow pH range (7.1-7.2) and is controlled by proton pumps and transporters.[15] Carbonate ions (HCO_3^-) and Na^+ are the main extracellular ions that compensate for changes in pH.[16] One of the most significant changed proteins in relation to the IDH1 mut appeared to be SLC4A4. This protein is a transporter of Na^+ and HCO_3^- into the cell and regulates intracellular pH.[17] The increase of SLC4A4 in IDH1 mut cells is a mechanism to correct intracellular pH, in accordance with the increased import of lactate into IDH1 mut glioma cells.

Changes in glutaminolysis in relation to cancer are not unique to the IDH1 mut and have been reported in relation to various cancer types.[18] A number of oncogenes and tumor suppressors like c-MYC, KRAS, and mTOR enhance or inhibit gene expression of enzymes involved in glutaminolysis.[18,19] In most tumors the Warburg effect (aerobic glycolysis) causes an increased lactate production and an extracellular export of lactate. Our data and findings of Lenting and co-workers indicate that in IDH1 mut gliomas lactate is actively imported into the cell in contrast to the Warburg effect. This results in metabolic changes specific to IDH1 mut gliomas and tailored to the tumor microenvironment in which large amounts of both glutamate and lactate are present.[20,21] In both IDH1 mut glioma tissues and glioma cell culture models with the IDH1 mutation, a decrease in both glutamate and lactate levels is reported.[22,23] These observations confirm our data and support an increased conversion of both lactate and glutamate into glioma cells with the IDH1 mut.

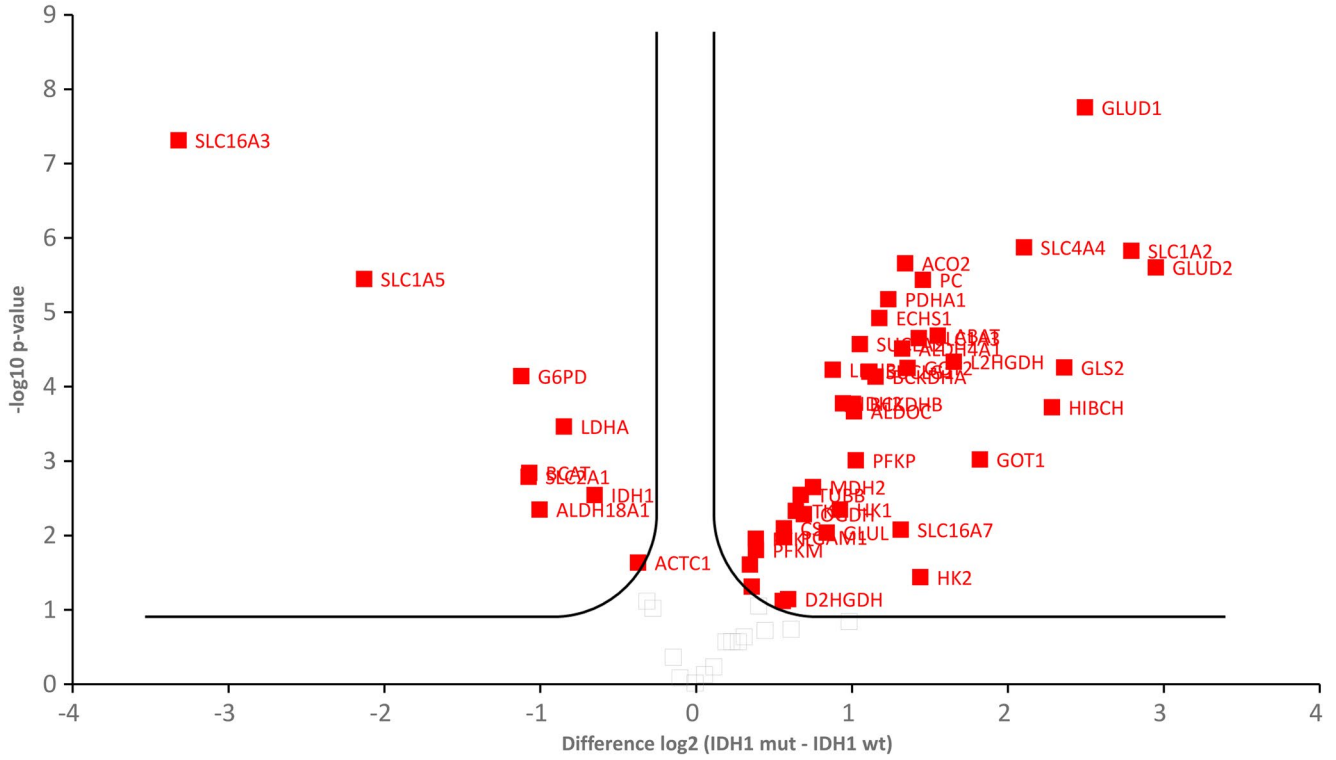

FIGURE 3 Volcano plot from PRM analyses. On the *x*-axis the difference between the two groups is indicated in a log2 value. The *y*-axis represents the −log10 of the *p*-value from the *t*-test. The significance cut-off is based on an FDR of 0.05 based on 250 randomizations of the dataset. The significant proteins are labeled and marked in red

A lack of significant changes in abundance of glycolysis enzymes corroborates with our gene expression data and the findings of Lenting and co-workers.[11] The glucose transporter (SLC2A3) and hexokinase 2 (HK2) were found downregulated in glioma samples with the IDH1 mut. We observed a decrease in protein level of the glucose transporter (SLC2A1), not the (SLC2A3) variant. A potential reason for discrepancies of our data from the transcriptomic data is the influence of non-tumor cells. The presence of erythrocytes or stromal cells in the glioma tissue samples could potentially influence the measured values to some extent. The influence of non-tumor cells on SLC2A1 abundance could be significant as SLC2A1 is highly abundant in fully matured erythrocytes and brain endothelial cells. GBM samples are more vascularized than lower-grade tumors and could for this reason contain more erythrocytes and endothelial cells. The abundance of hexokinase variants, HK1 and HK2, was increased in IDH1 mut glioma. Higher levels of HK1 abundance in low-grade gliomas is associated with normal oxidative respiration and this is indicative of a decrease in aerobic glycolysis.[24] The data indicate that lactate is imported in IDH1 mut brain tumor cells. Lactate is used for the production of pyruvate which is shuttled into the TCA cycle resulting in an increase in oxidative respiration. Oppermann et al have already shown that extracellular pyruvate can fuel the TCA cycle.[25] In cell culture experiments of U87 (IDH1 wt) cells, it was observed that glucose can be replaced by pyruvate. In these cells, pyruvate is imported and the TCA-cycle intermediates citrate, α-ketoglutarate, and succinate are increased, indicative of the utilization of extracellular pyruvate in the TCA cycle. In addition, in vivo experiments have shown that extracellular lactate may be used as an energy source in the human brain.[26] Expression levels of HK2 increase with glioma grade and the highest RNA expression and protein levels are found in GBM.[24,27,28] However, we were unable to confirm this by proteomics. In GBM cell lines it was shown that knocking down HK2 results in inhibition of the aerobic glycolysis leading to an increase in normal oxidative respiration and a decrease in lactate production. HK2 is crucial for the Warburg effect, increasing aerobic glycolysis. Our findings corroborate this observation and indicate that aerobic glycolysis is increased in the IDH1 wt glioma, in contrast to IDH mut glioma.

Lenting and co-workers showed that the GABA shunt is upregulated in IDH1 mut glioma.[11] ALDH5A1 is one of the proteins with the largest difference in abundance between IDH1 wt and IDH mut gliomas in the DDA analyses. ALDH5A1 converts succinic semi-aldehyde into succinate and is as such part of the GABA shunt. In addition, two other enzymes of the GABA shunt, DCE1 and ABAT, were investigated. For DCE1 we were not able to obtain quantitative data, while for ABAT we observed a significant increase in IDH1 mut gliomas indicating that the GABA shunt is upregulated. The increase in the GABA-shunt protein

TABLE 2 Results of volcano plot analyses comparing IDH1 wt (GBM) with IDH1 mut (astrocytoma and oligodendroglioma)

Gene name	Significant FDR < 0.05	*p*-value	Ratio IDH1 mut/IDH1 wt
GLUD1	+	2.06E-11	5.92
SLC16A3	+	5.88E-11	0.06
SLC1A2	+	2.37E-10	8.99
SLC4A4	+	2.74E-10	5.05
ACO2	+	2.89E-10	2.78
PC	+	3.25E-10	3.11
GLUD2	+	4.44E-10	8.11
ABAT	+	1.10E-09	3.67
PDHA1	+	1.28E-09	2.51
ECHS1	+	1.59E-09	2.41
SLC1A3	+	1.89E-09	3.07
SUCLA2	+	2.83E-09	2.40
SUCLG1	+	3.58E-09	2.66
SLC1A5	+	4.51E-09	0.17
LDHB	+	5.96E-09	2.19
ALDOC	+	1.15E-08	2.80
IDH2	+	1.39E-08	2.11
L2HGDH	+	1.84E-08	3.08
GOT2	+	1.98E-08	2.62
G6PD	+	2.14E-08	0.47
HIBCH	+	2.88E-08	5.12
BCKDHB	+	6.17E-08	1.96
GLS2	+	6.86E-08	5.31
PFKP	+	7.24E-08	2.33
BCKDHA	+	1.09E-07	2.04
GOT1	+	1.36E-07	4.16
ALDH4A1	+	2.50E-07	2.19
LDHA	+	5.22E-07	0.53
TUBB	+	9.09E-07	1.74
PGAM1	+	9.91E-07	1.79
MDH2	+	1.25E-06	1.78
GLUL	+	1.37E-06	2.14
PFKL	+	1.96E-06	1.46
HK1	+	3.02E-06	2.10
BCAT	+	3.23E-06	0.47
TKT	+	3.77E-06	1.64
PFKM	+	3.83E-06	1.46
CS	+	5.09E-06	1.61
SLC16A7	+	7.65E-06	3.08
OGDH	+	9.25E-06	1.70
ALDH18A1	+	2.69E-05	0.48
SLC2A1	+	3.34E-05	0.54
HK2	+	4.78E-05	3.57
PGD	+	3.62E-04	0.74
MLYCD	+	4.06E-04	1.66
SDHA	+	7.13E-04	1.37
ENO1		1.95E-03	1.30
ACACA	+	3.17E-03	1.41
FH	+	3.61E-03	1.58
OAT	+	6.13E-03	1.44
D2HGDH	+	1.04E-02	1.56
GLS	+	2.12E-02	2.32
TPI1	–	2.57E-02	1.26
SDHB	–	3.05E-02	1.36
SUCLG2	–	5.12E-02	1.33
IDH1	–	2.29E-01	0.78
PGK1	–	2.63E-01	1.23
SLC2A3	–	3.38E + 01	1.44
ACTC1	–	3.52E + 01	0.88
GPI	–	7.15E + 01	1.17
PGLS	–	7.01E + 02	0.89
PKM	–	1.14E + 03	1.11
FASN	–	9.08E + 05	1.17
GAPDH	–	2.46E + 07	0.95

ABAT, which introduces additional succinate to the TCA cycle, explains the increased levels of the TCA-cycle enzymes that further process succinate. Aldehyde dehydrogenase 6 (ALDH6A1) is involved in the valine and thymine catabolism and we found a significant change in abundance in relation to the IDH1 mutation in the DDA analysis.[29] For this reason, amino acid catabolism was investigated in our targeted analyses. The enzymes involved in valine, leucine, and isoleucine catabolism (ECHS1, BCKHA, BCKHB, and HIBCH) were all significantly higher in abundance in IDH1 mut glioma samples, confirming the increase in amino acid catabolism. Glutamate and α-ketoglutarate play central roles in the catabolism of these amino acids. Proline catabolism is affected and both OAT and ALDH4A1 levels are increased, indicating that proline is converted into glutamate. In addition, the transporters of glutamate, alanine, serine, cysteine, and threonine (SLC1A2, SLC1A3, and SLC1A4) are increased. Taken together, this makes it likely that amino acid catabolism is increased for anaplerotic feeding of the TCA cycle. In addition, the presented data indicate that in IDH1 mut gliomas, compensation mechanisms are being activated to produce extra TCA-cycle metabolites to keep the TCA cycle active. It is, however, striking that the glycolysis route that fuels the TCA cycle is not increased (the glucose importer SLC2A3 RNA expression is even decreased[11]). The obstructed catabolism of glucose in IDH1 mut gliomas was reported before.[11,22,30] By metabolic flux experiments

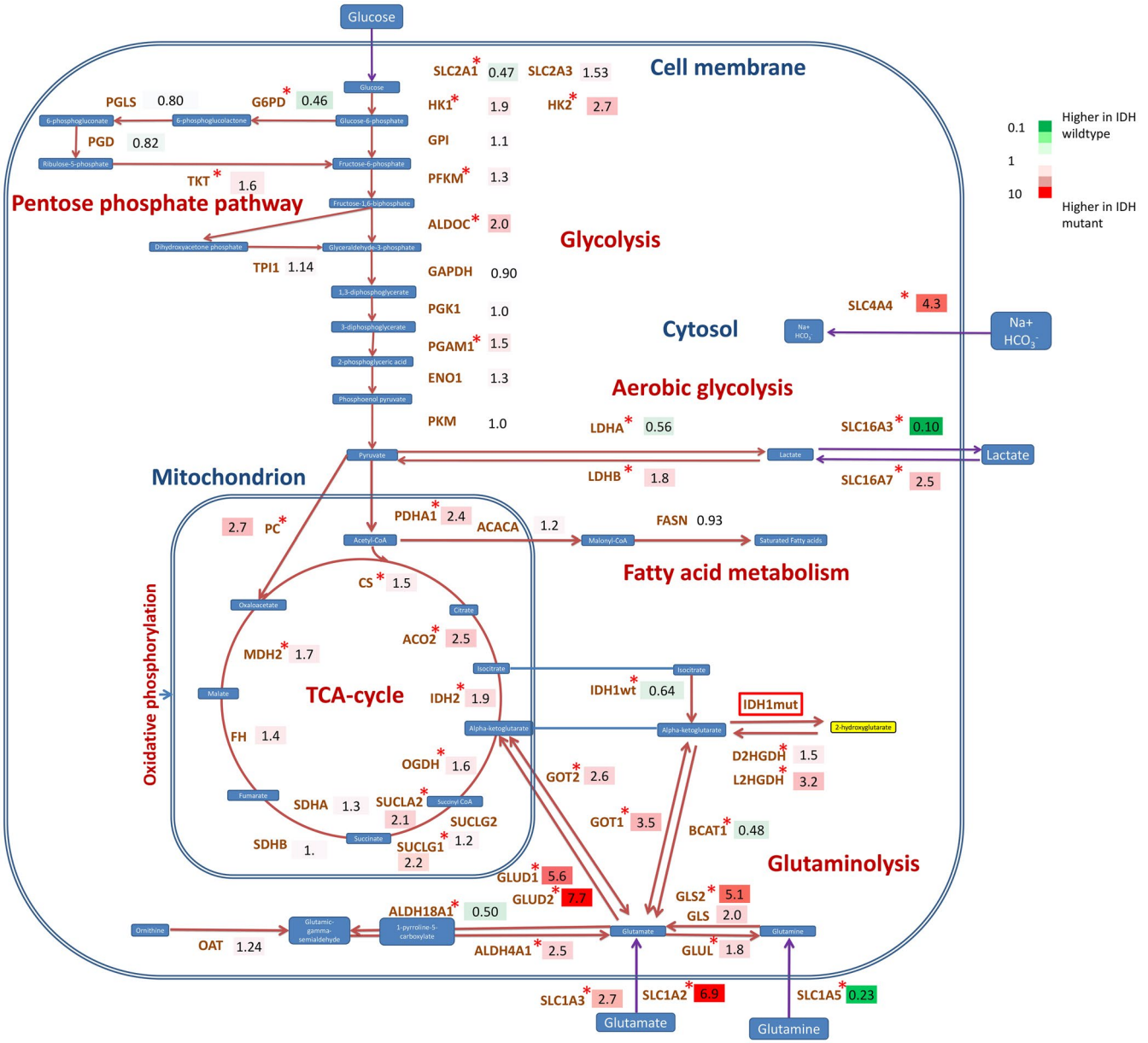

FIGURE 4 Overlay of protein abundance data with metabolic pathways of the glycolysis, pentose phosphate pathway, TCA cycle, and glutaminolysis. The red arrows indicate an enzymatic reaction and the purple arrows represent transport of a metabolite over the cell membrane. The number next to each protein in the metabolic map represents the ratio between the IDH1 wt group and IDH1 mut group. A red asterisk indicates that the difference between the two groups is significant based on the volcano plot analyses with an FDR correction of 0.05 based on 250 randomizations of the data. The glutaminolysis and the aerobic glycolysis appear to be affected mostly by the IDH1 mut

in an IDH1 R132H patient-derived xenograft (PDX) it was shown that glucose is scarcely used as the carbon source for either α-ketoglutarate or 2-hydroxy-glutarate, indicative of the use of alternative carbon sources for the production of these metabolites to fuel the TCA-cycle.[30] Recently by pH and oxygen-sensitive MRI imaging of glioma patients, large differences in the tumor microenvironment of IDH1 wt and mut gliomas are observed. The authors suggest that these changes indicate that in IDH1 mut tumors the aerobic glycolysis is less active and the TCA cycle is more active which is in agreement with our findings.[31]

Our data and previously acquired RNA expression data are all an indirect read-out of the metabolome. A direct measurement of the metabolome itself could potentially be more accurate. The disadvantages of a metabolomics study are that fresh-frozen tissues are required. In addition, metabolites are often involved in different chemical reactions which make it difficult to identify the exact reaction in which

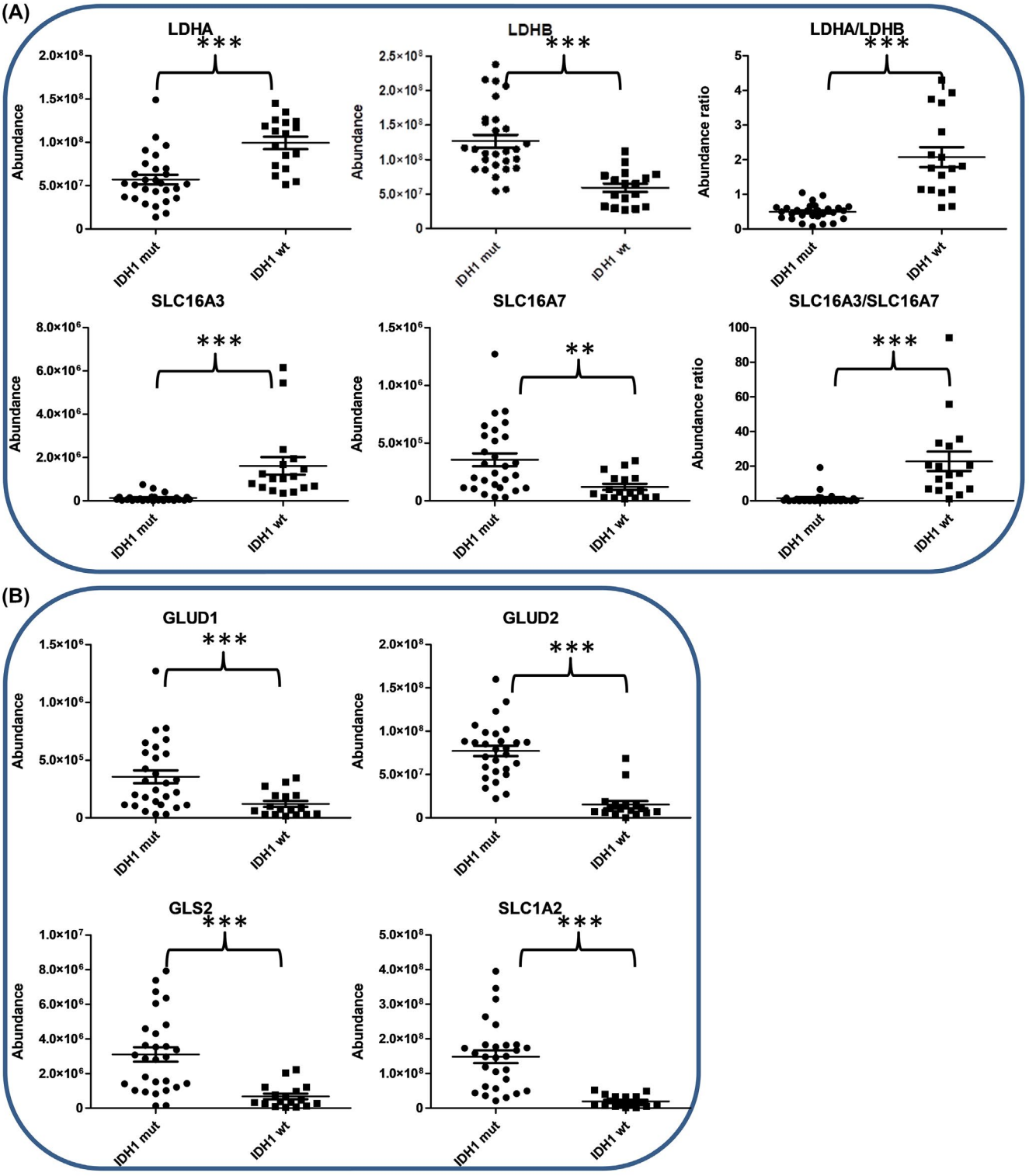

FIGURE 5 Abundance plots of the aerobic glycolysis and glutaminolyses based on PRM analyses. Abundance plots for panel (A) aerobic glycolysis and panel (B) glutaminolyses. In addition to the abundance plots of LDHA, LDHB, SLC16A3, and SLC16A7, the ratio between LDHA and LDHB and between SLC16A3 and SLC16A7 are displayed (panel A). The ratios indicate that predominantly in the IDH1 mut group lactate is transported into the cell and converted into pyruvate. The importer of glutamate (SLC1A2) and GLUD1 and GLUD2 (enzymes that convert glutamate into α-ketoglutarate) is increased in the IDH1 mut group (panel B). In all plots, the mean and SEM (standard error of the mean) are indicated for both groups, statistical differences (*t*-test) are indicated by asterisk's (***P*-value < .001, ****P*-value < .0001)

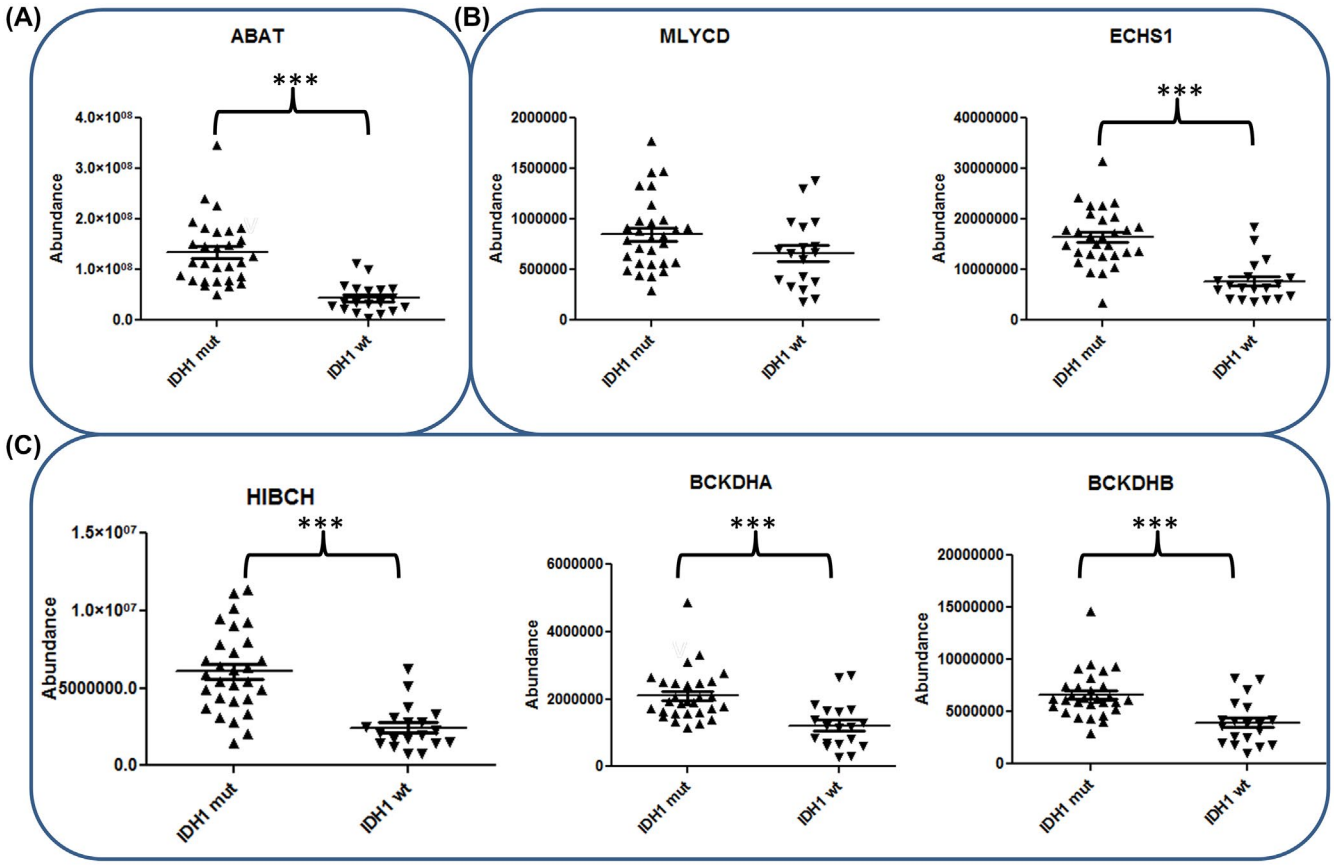

FIGURE 6 Abundance plots based on PRM analyses. Abundance plots based on PRM analyses for ECHS1 and MLYCD (fatty acid metabolism) panel (A) for BCKHA, BCKHB, and HIBCH (valine, leucine, and isoleucine degradation) panel (B), and for ABAT (GABA shunt) panel (C). For all plots in the three panels the IDH1 mut group is compared with the IDH1 wt group. Statistical differences (*t*-test) are indicated by asterisks (****P*-value < .001). All proteins were found to be statistically different except for MLYCD. For all analysis the mean value with the SEM is indicated

changes occur. The protein content of a sample is usually less effected by sample collection procedures and can be extracted from FFPE material of which large collections are mostly available. Furthermore, enzymes catalyze very specific reactions; often (iso-)forms exist which are specific for a cellular compartment (mitochondrial, cytosolic) or tissue type. This information cannot be extracted from a metabolomics study and intra- and extracellular concentrations of metabolites cannot be distinguished. For these reasons we have chosen a proteomics approach, although this represents an indirect way to measure enzymatic activity. In this respect, we note that in an earlier study it was shown that RNA expression could be used as a surrogate to observe differences in the metabolism.[32] As enzymes themselves are one step closer to the metabolome, their abundances should better represent the activity of metabolic processes. Our findings, however, need to be confirmed on the metabolic level, the lack of IDH1 mutant cellular and preclinical models and the appropriate biological context of the existing models makes it difficult to translate such findings to the patient situation.[33] The altered metabolic processes probably largely depend on the microenvironment of the tumor cells resulting in rather large assumptions to translate findings from cell culture models to the in vivo situation. For this reason models that are closer to the in vivo situation, for instance, glioma PDX models have an advantage.[34] A relative large panel of inhibitors that target enzymes or transporters of the glutamate metabolism exist.[19] The inhibitors open possibilities to target these enzymes in metabolic flux experiments in IDH1-mutated glioma PDX models to validate the findings in this study. In addition are improvements made in MRI imaging which allow in vivo metabolic profiling of tumors.[31,35]

In conclusion, in IDH1 mut glioma significant differences in specific enzymes of the glutaminolysis and aerobic glycolysis are found. This proteomics study confirms and extends on earlier findings at the RNA expression level. The observations in IDH mut glioma are independent of tumor grade or molecular subtype of the tumor and affect predominantly the abundance of enzymes related to glutaminolysis. Based on these results we propose that the import of glutamate into IDH1 mut cells is increased as well as

the conversion of glutamate into α-ketoglutarate. Enzymes that convert proline, valine, leucine, and isoleucine into glutamate are also increased. Furthermore, the transport of lactate and the enzymes involved in the subsequent conversion into α-ketoglutarate are increased. The increased intake of lactate results in intracellular acidification which is most likely compensated by an increase in the bicarbonate transporter (SLC4A4). The metabolism seems to be rewired to produce additional α-ketoglutarate to preserve the TCA cycle as a survival mechanism for IDH1 mut gliomas. Further validation including metabolic flux experiment is required. The presented data aids in a better understanding of the role of the IDH1 mutation in glioma metabolism and can generate ideas how drugs can be designed to interfere with the specific energy requirements in IDH1 mut and IDH1 wt glioma.

ACKNOWLEDGMENTS

The mass spectrometry equipment used for this publication is (partly) financed by the Netherlands Organisation for Scientific Research (NWO) infrastructure grant number 1631. This work has received funding from the Eurostars-2 joint program with co-funding from the European Union Horizon 2020 research and innovation program (Eurostars project 10688 (GlioPhos)) and by the British Brain Tumour Charity (GN-000540).

CONFLICT OF INTEREST

The authors have no conflicts of interest to declare.

AUTHOR CONTRIBUTIONS

L. J. M. Dekker, T. M. Luider, and J. M. Kros designed the study; J. M. Kros and D. A. N. Mustafa collected the sample; J. M. Kros, D. A. N. Mustafa, and F. Grevers collected clinical information; J. M. Kros performed histological review; L. J. M. Dekker, C. Jurriëns, and S. Wu performed experiments; L. J. M. Dekker analyzed the Data; L. J. M. Dekker, D. A. N. Mustafa, C. Jurriëns, S. Wu, P. C. Burgers, P. A. E. Sillevis Smitt, J. M. Kros, and T. M. Luider discussed and wrote the manuscript. All authors read and approved the final manuscript.

REFERENCES

1. Cohen AL, Holmen SL, Colman H. IDH1 and IDH2 mutations in gliomas. *Curr Neurol Neurosci Rep*. 2013;13:345.
2. Yan H, Parsons DW, Jin G, et al. IDH1 and IDH2 mutations in gliomas. *N Engl J Med*. 2009;360:765-773.
3. Zhao H, Heimberger AB, Lu Z, et al. Metabolomics profiling in plasma samples from glioma patients correlates with tumor phenotypes. *Oncotarget*. 2016;7:20486-20495.
4. Bogdanovic E. IDH1, lipid metabolism and cancer: shedding new light on old ideas. *Bba-Gen Subjects*. 2015;1850:1781-1785.
5. Grassian AR, Parker S, Davidson S, et al. IDH1 mutations alter citric acid cycle metabolism and increase dependence on oxidative mitochondrial metabolism. *Cancer Res*. 2014;74:3317-3331.
6. Suijker J, Oosting J, Koornneef A, et al. Inhibition of mutant IDH1 decreases D-2-HG levels without affecting tumorigenic properties of chondrosarcoma cell lines. *Oncotarget*. 2015;6:12505-12519.
7. Kopinja J, Sevilla RS, Levitan D, et al. A brain penetrant mutant IDH1 inhibitor provides in vivo survival benefit. *Sci Rep*. 2017;7:13853.
8. Turcan S, Rohle D, Goenka A, et al. IDH1 mutation is sufficient to establish the glioma hypermethylator phenotype. *Nature*. 2012;483:479-483.
9. Mondesir J, Willekens C, Touat M, de Botton S. IDH1 and IDH2 mutations as novel therapeutic targets: current perspectives. *J Blood Med*. 2016;7:171-180.
10. Mustafa DAN, Swagemakers SM, Buise L, van der Spek PJ, Kros JM. Metabolic alterations due to IDH1 mutation in glioma: opening for therapeutic opportunities? *Acta Neuropathol Commun*. 2014;2:6.
11. Lenting K, Khurshed M, Peeters TH, et al. Isocitrate dehydrogenase 1–mutated human gliomas depend on lactate and glutamate to alleviate metabolic stress. *FASEB J*. 2019;33:557-571.
12. van Lith SA, Navis AC, Verrijp K, et al. Glutamate as chemotactic fuel for diffuse glioma cells: are they glutamate suckers? *Biochim Biophys Acta*. 2014;1846:66-74.
13. Louis DN, Perry A, Reifenberger G, et al. The 2016 World Health Organization classification of tumors of the central nervous system: a summary. *Acta Neuropathol*. 2016;131:803-820.
14. Dekker LJM, Zeneyedpour L, Snoeijers S, Joore J, Leenstra S, Luider TM. Determination of site-specific phosphorylation ratios in proteins with targeted mass spectrometry. *J Proteome Res*. 2018;17:1654-1663.
15. Gautier EF, Ducamp S, Leduc M, et al. Comprehensive proteomic analysis of human erythropoiesis. *Cell Rep*. 2016;16:1470-1484.
16. Gallagher FA, Kettunen MI, Day SE, et al. Magnetic resonance imaging of pH in vivo using hyperpolarized 13C-labelled bicarbonate. *Nature*. 2008;453:940.
17. Soleimani M, Burnham CE. Physiologic and molecular aspects of the Na+:HCO3- cotransporter in health and disease processes. *Kidney Int*. 2000;57:371-384.
18. Lifeng Y, Sriram V, Deepak N. Glutaminolysis: a hallmark of cancer metabolism. *Annu Rev Biomed Eng*. 2017;19:163-194.
19. Altman BJ, Stine ZE, Dang CV. From Krebs to clinic: glutamine metabolism to cancer therapy. *Nat Rev Cancer*. 2016;16:619-634.
20. Riske L, Thomas RK, Baker GB, Dursun SM. Lactate in the brain: an update on its relevance to brain energy, neurons, glia and panic disorder. *Ther Adv Psychopharmacol*. 2017;7(2):85-89.
21. Zhou Y, Danbolt NC. Glutamate as a neurotransmitter in the healthy brain. *J Neural Transm*. 2014;121(8):799-817.
22. Izquierdo-Garcia JL, Viswanath P, Eriksson P, et al. Metabolic reprogramming in mutant IDH1 glioma cells. *PLoS One*. 2015;10:e0118781.
23. Zhou L, Wang Z, Hu C, et al. Integrated metabolomics and lipidomics analyses reveal metabolic reprogramming in human glioma with IDH1 mutation. *J Proteome Res*. 2019;18:960-969.
24. Wolf A, Agnihotri S, Micallef J, et al. Hexokinase 2 is a key mediator of aerobic glycolysis and promotes tumor growth in human glioblastoma multiforme. *J Exp Med*. 2011;208:313-326.
25. Oppermann H, Ding Y, Sharma J, et al. Metabolic response of glioblastoma cells associated with glucose withdrawal and pyruvate substitution as revealed by GC-MS. *Nutr Metab (Lond)*. 2016;13:70.

26. Boumezbeur F, Petersen KF, Cline GW, et al. The contribution of blood lactate to brain energy metabolism in humans measured by dynamic 13C nuclear magnetic resonance spectroscopy. *J Neurosci*. 2010;30:13983-13991.
27. Vartanian A, Agnihotri S, Wilson MR, et al. Targeting hexokinase 2 enhances response to radio-chemotherapy in glioblastoma. *Oncotarget*. 2016;7:69518-69535.
28. Liu H, Liu N, Cheng Y, et al. Hexokinase 2 (HK2), the tumor promoter in glioma, is downregulated by miR-218/Bmi1 pathway. *PLOS One*. 2017;12(12):e0189353.
29. Marcadier JL, Smith AM, Pohl D, et al. Mutations in ALDH6A1 encoding methylmalonate semialdehyde dehydrogenase are associated with dysmyelination and transient methylmalonic aciduria. *Orphanet J Rare Diseases*. 2013;8(1):98.
30. Fack F, Tardito S, Hochart G, et al. Altered metabolic landscape in IDH-mutant gliomas affects phospholipid, energy, and oxidative stress pathways. *EMBO Mol Med*. 2017;9:1681-1695.
31. Yao J, Chakhoyan A, Nathanson DA, et al. Metabolic characterization of human IDH mutant and wild type gliomas using simultaneous pH- and oxygen-sensitive molecular MRI. *Neuro-Oncology*. 2019;21:1184-1196.
32. Khurshed M, Molenaar RJ, Lenting K, Leenders WP, van Noorden CJF. In silico gene expression analysis reveals glycolysis and acetate anaplerosis in IDH1 wild-type glioma and lactate and glutamate anaplerosis in IDH1-mutated glioma. *Oncotarget*. 2017;8:49165-49177.
33. Parker SJ, Metallo CM. Metabolic consequences of oncogenic IDH mutations. *Pharmacol Ther*. 2015;152:54-62.
34. Lenting K, Verhaak R, Ter Laan M, Wesseling P, Leenders W. Glioma: experimental models and reality. *Acta Neuropathol*. 2017;133(2):263-282.
35. Fuss TL, Cheng LL. Metabolic imaging in humans. *Top Magn Reson Imaging*. 2016;25:223-235.

SUPPORTING INFORMATION

Additional supporting information may be found online in the Supporting Information section.

How to cite this article: Dekker LJM, Wu S, Jurriëns C, et al. Metabolic changes related to the IDH1 mutation in gliomas preserve TCA-cycle activity: An investigation at the protein level. *The FASEB Journal*. 2019;00:1–12. https://doi.org/10.1096/fj.201902352R